Deliverable 6.6 Report on the role winter convection in controlling the basin-scale C budget

Lindemann, Christian; Grosse, Fabian; Backhaus, Jan O.

Publication date:
2014

Document Version
Publisher's PDF, also known as Version of record

EURO-BASIN
BASIN SCALE ANALYSIS, SYNTHESIS AND INTEGRATION

SEVENTH FRAMEWORK PROGRAMME THEME 7 Environment

Collaborative project (Large-scale Integrating Project)

Project no: 246 933

Project Acronym: EURO-BASIN

Project title: European Basin-scale Analysis, Synthesis and Integration

Deliverable 6.6 Report on the role winter convection in controlling the basin-scale C budget

Contributors: Christian Lindemann (DTU Aqua),
Fabian Grosse (UHam), Jan O. Backhaus (UHam)

Due date of deliverable: Nov 2013
Actual submission date: Jan 2014
Organisation name of the lead contractor of this deliverable: DTU Aqua

Start date of project: 31.12.2010 Duration: 48 months
Project Coordinator: Michael St John, DTU Aqua

Project co-funded by the European Commission within the Seventh Framework Programme,
Theme 6 Environment

		Dissemination Level
PU	Public	
PP	Restricted to other programme participants (including the Commission)	X
RE	Restricted to a group specified by the consortium (including the Commission)	
CO	Confidential, only for members of the consortium (including the Commission)	

Deliverable 6.6 Report on the role winter convection in controlling the basin-scale C budget

is a contribution to T6.2.4: Development of CIBM and evaluation of parameterisations. CIBM will be run in selected regions with T-S-profiles and external met-forcing from our basin-models. Its predictions will be used to optimise the 'biological' parameterisation of convection. This work will be informed by fieldwork undertaken in WP's 2&4 on the METEOR convection cruise. The CIBM, thus, serves as a benchmark for checking the quality of the parameterisation. These parameterisations will then be implemented in the ¼ coupled physical-biological models of basin to quantify the role of the winter biomass in terms of the carbon- or CO2-budget in comparison to 'conventional' models.

Responsible: DTU, UHAM
Start month 1, end month 36

Executive Summary:

The goal of T6.6 is to increase your knowledge about the effects of the winter phytoplankton in the North Atlantic on the annual carbon budget. It has been hypothesized that deep convection plays a major role in maintaining phytoplankton cells within the mixed layer by superimposing sinking and frequently exposing them to the euphotic zone, thus sustaining a viable phytoplankton stock. Due to the hydrostatic nature of the physical models commonly used in ecosystems models, a parameterisation of the relation between winter phytoplankton and deep convection is needed in order to evaluate the standing stock and the related carbon export.

To inform a meaningful parameterisation, a coupled non-hydrostatic Individual-Based phytoplankton model (CIBM) was used to estimate the bio-physical interplay. A simple parameterisation was implemented into an ecosystem model. In agreement with field observations, both the CIBM and the implemented parameterisation predicted a sustained viable phytoplankton population. The parameterisation of winter growth improved the fit with field data significantly.

This work informs WP8 about the potential impacts of climate change and other anthropogenic influences on the winter carbon budget in the North Atlantic.

Relevance to the project & potential policy impact:

The outputs of the simulations will help to create reliable ecosystem estimates of winter phytoplankton stock and its relation to carbon export. This work will allow a better evaluation of the potential impacts of climate change no the carbon budget of the North Atlantic.

Access to Data and/or model code (where relevant):

Model code and raw model output can be requested from Christian Lindemann (chrli@aqua.dtu.dk). Access is restricted simply to allow developer to complete PhD Thesis.

How to cite the contents of the report:

Grosse, F., C. Lindemann, J. Paetsch, J.O. Backhaus. The influence of deep winter convection on primary production: a parameterisation using a hydrostatic three-dimensional biogeochemical model, Subm. to Journal of Marine Systems

Report:

The purpose of the deliverable is to document the development, validation and implementation of (a) a phytoplankton CIBM into a 2D non-hydrostatic convection model, (b) the 'phyto-parameterisation' into an ecosystem model and (c) to access the importance of the winter phytoplankton for the carbon budget.

Studies suggest that ocean convection plays a key role in primary production during winter (e.g. Backhaus et al., 1999; Wehde et al., 2001). In 1999, Backhaus et al. hypothesised a direct link between ocean convection and primary production termed ‘phytoconvection’.

They suggested that the vertical motion of the convective plumes can cause phytoplankton particles to regularly re-enter the euphotic zone allowing to grow, and thus, balancing their loss terms. This relation is supported by modelling and observational studies (Backhaus et al., 2003; Wehde and Backhaus, 2000; D’Asaro, 2008).

Biological models commonly are coupled to hydrostatic physical models and therefore are unable to resolve convective motion explicitly. In order to estimate stratification under the influence of convection, parameterisations are used. These parameterisations are usually only applied to the physics, while the biological compartment is modelled using the classical phytoplankton-bulk-biomass approach.

This approach does not allow for the convective vertical displacement of cells, thus the influence of deep convection on phytoplankton dynamics cannot be captured in common ecosystem models. Therefore a full process model description requires both a non-hydrostatic convection model for the physics and an individual based model (IBM) to describe the biology.

1. Convection Individual-Based-Model (CIBM)

The model consists of a physical 2D non-hydrostatic convection model and a biological Individual-Based-Model for phytoplankton.
An extended description of the CIBM (incl. Equations) can be found in Appendix I.

1.1 Non-hydrostatic convection model

The convection model (CM) is based on the non-hydrostatic Boussinesq-equations for an incompressible fluid and has previously been utilized in several numerical studies of convection (e.g. Backhaus et al. 1999; Kämpf and Backhaus 1998; Wehde and Backhaus 2000; Wehde et al. 2001). The model describes a 2,5-dimensional ocean slice with cycling boundary conditions. For a full description of the model reference is made to Kämpf and Backhaus (1998) and Wehde and Backhaus (2000). The model differs from earlier applications in that seawater-density is calculated using the equation of state by McDougall et al. (2003).

1.2 Phytoplankton Individual-Based-Model

The biological IBM describes the dynamics of the phytoplankton cells within the ocean slice. In the CM the individual cells are represented as Lagrangian particles influenced by their own sinking rate and hydrodynamics (in the same manner as water). Phytoplankton growth during winter in the North Atlantic is driven by the availability of PAR with non-limiting nutrient levels and minimal grazing pressure. Hence nutrients and grazing are not included in this model. Light-dependent photosynthesis (μ) is calculated according to Jassby & Platt (1976), with a temperature-dependency according to Bissinger et al. (2008). Adopting the approach by Sakshaug et al. (1989), the respiration rate is assumed to be 12% of the growth rate. Sakshaug et al (1989) based this parameterisation on findings by Falkowski and Owens (1980). They showed that light/shade adapted phytoplankton cells acclimatise their dark respiration rate to different light regimes proportional to their gross primary production. The sinking rate of each cell is calculated for each time step, based on the concept by Waite et al. (1992), who coupled the sinking rate to the overall metabolic state of the cell.

1.3 CIBM simulations

The model simulations describe phytoplankton cells being mixed in turbulent convective regime under meteorological forcing. Two simulations at different stations and times of year have been made to test the CIBM as follows;

1.3.1 62°N 22°W

Experiment: For the meteorological forcing we used the Global Reanalysis ERA-Interim dataset provided by the European Centre for Medium-Range Weather Forecasts (http://www.ecmwf.int/).

The initial conditions as well as chlorophyll data for validation were available from ARGO floats (downloaded from *www.coriolis.eu.org/*). The simulation was run from 04th February 2010 to 17th March 2010, the first 5 days were considered as spin-up. 40.000 Lagrangian tracers were randomly distributed from 10 to 300 m depth at the beginning of the simulation.

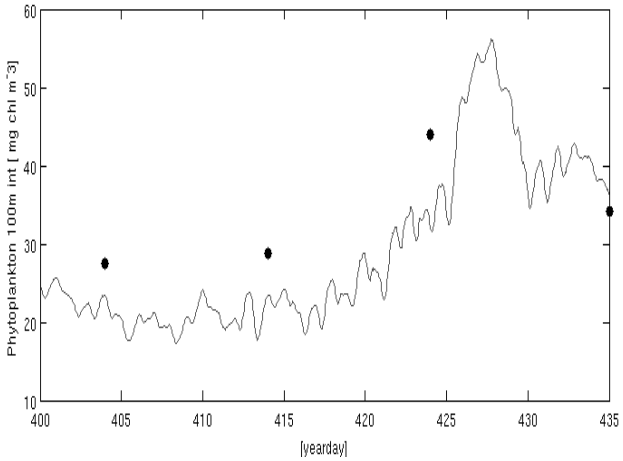

Figure 1 *Integrated (0-100 m) chlorophyll from the model simulation (line) and ARGO float measurements (dots)*

Results:

The model run simulates condition of deep winter mixing in the North Atlantic over one month. In general the 100m integrated estimated biomass is about 5 mg chl m^{-3} too low but captures the dynamics of the system well (Fig. 1). More intensive mixing (Fig. 2b) coincided with a stronger heat loss at the surface (Fig.2a), while the temperature was largely unaffected by short-term dynamics (Fig. 2c) showing a cooling trend during the time simulated. Phytoplankton biomass increases, in agreement with ARGO measurements, during the time of simulation, peaking at around yearday 60 (Fig. 2d). The subsequent increase in surface heat loss and the related intensive convection lead to the cells being mixed over the whole mixed layer, thus decreasing surface chlorophyll.

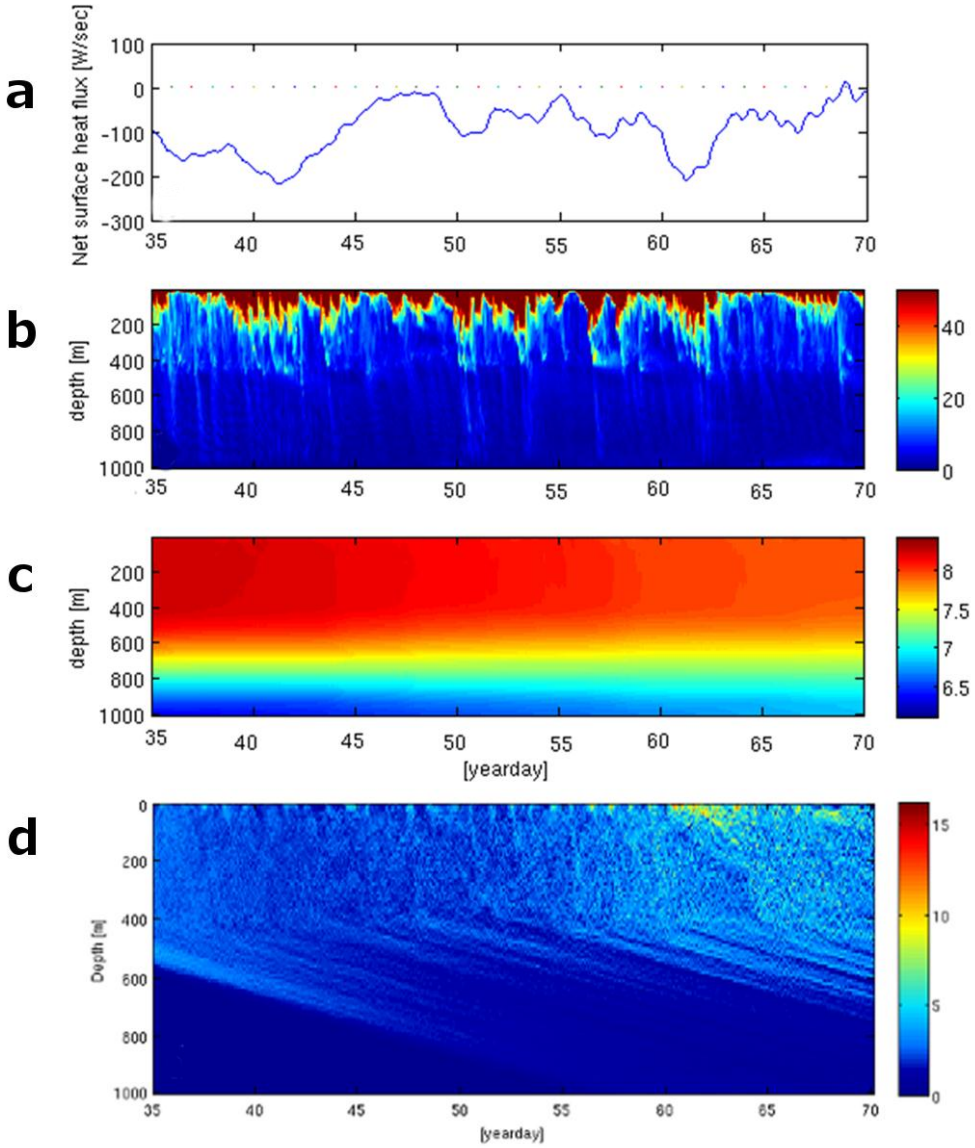

Figure 2 *(a) Time series of net surface heat flux [W m^{-2}] and Hovmoeller diagram showing (b) turbulence (log scale) (c) temperature [°C] and (d) phytoplankton concentration [mg Chl m^{-3}] over the course of the* simulation.

1.3.2 Station M (66°N 02°E)

Experiment: Three-hourly meteorological forcing for this simulation was kindly provided by the Norwegian Meteorological Office (METNO). The initial conditions as well as chlorophyll data for validation were kindly provided by X. Irigoien. The simulation was run from the 10th of April 1997 to 16th of May 1997, the first 5 days were considered as spin-up. 40.000 Lagrangian tracers were randomly distributed from 10 to 300 m depth at the beginning of the simulation.

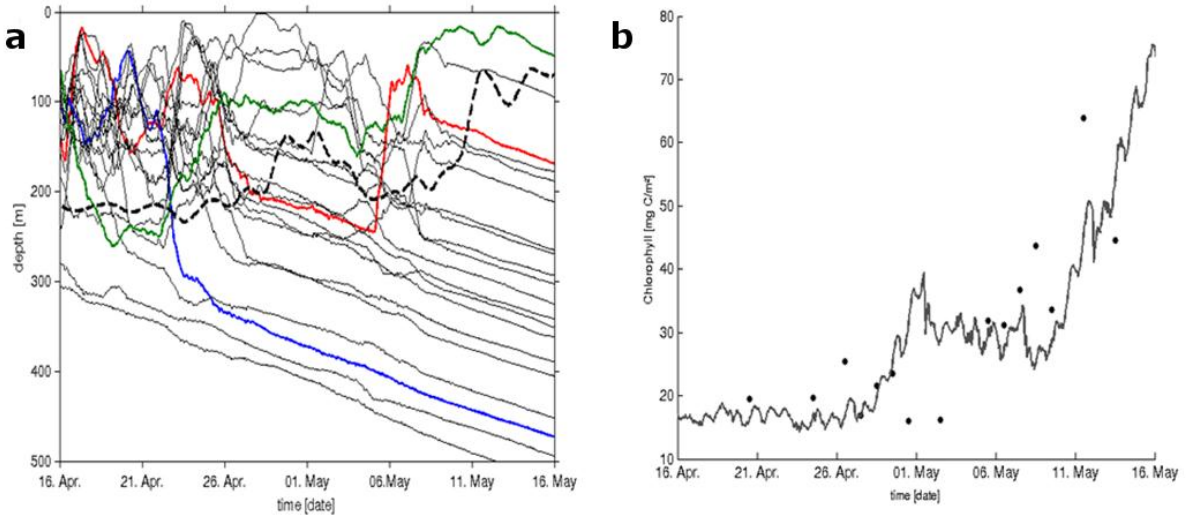

Figure 3 *(a) Examples of particle trajectories as simulated by the coupled Convection-Individual-Based model. Colored particle tracks are examples of possible different fades. The blue track particle sinking out of the convective mixed layer (dashed line) The red marks a particle leaving and re-entering the CML The green marked particle stays within the CML during the course of the simulation. (b) Comparison of the observed (dots) and simulated (line) integrated chlorophyll a values over the upper 100 of the water column from mid-April to mid-May at Ocean Weather station 'Mike'.*

Results:

Individual tracers are mixed within the convective mixed layer (CML) with sedimentation (tracer dropping out of the CML) occurring throughout the whole simulation (Fig. 3a). The beginning of the simulation is characterized by strong heat loss at the surface, indicated by the negative net surface heat flux (Fig. 4a), with minimal values of around -350 W m^{-2}. The resultant stimulated mixing can be approximated by the turbulent exchange coefficient estimated by the CM (Fig. 4b). This period of strong mixing is followed by a decline in net surface heat loss (-100 to 70 W m^{-2}). Accordingly, the mixed layer depth (MLD, Fig. 4e), defined as the depth where the difference in temperature between the depth and 10 m below the surface exceeds 0.8°C, shows a reduction from around 230 m to 150 m. Around 04th May the net surface heat flux drops again to -200 W m^{-2} inducing enhanced convective activity and lowering the MLD back to around 200 m. Towards the end of the simulation (~09th May) the net surface heat flux turns positive and stabilizes at around 150 W m^{-2}. This leads to a strong reduction in mixing which is followed by a stabilization of the water column (~12th May) as indicated by the temperature profile (Fig. 4c) and the estimated MLD, which retreated to around 75 m. Changes in MLD and convection coincide with the change in surface temperatures, which shows a warming trend throughout the simulation (Fig. 3c). The

reduction in MLD occurs about two to three days after the convection stopped. Phytoplankton biomass starts to increase after the convective mixing shut down but before stratification set in (Fig. 4). In general the model manages to capture the biomass as well as the general dynamics of the winter phytoplankton in comparison with observations (Irigoien et al. 1998; Niehoff et al. 1999) available for the upper 100 meters (Fig. 3b).

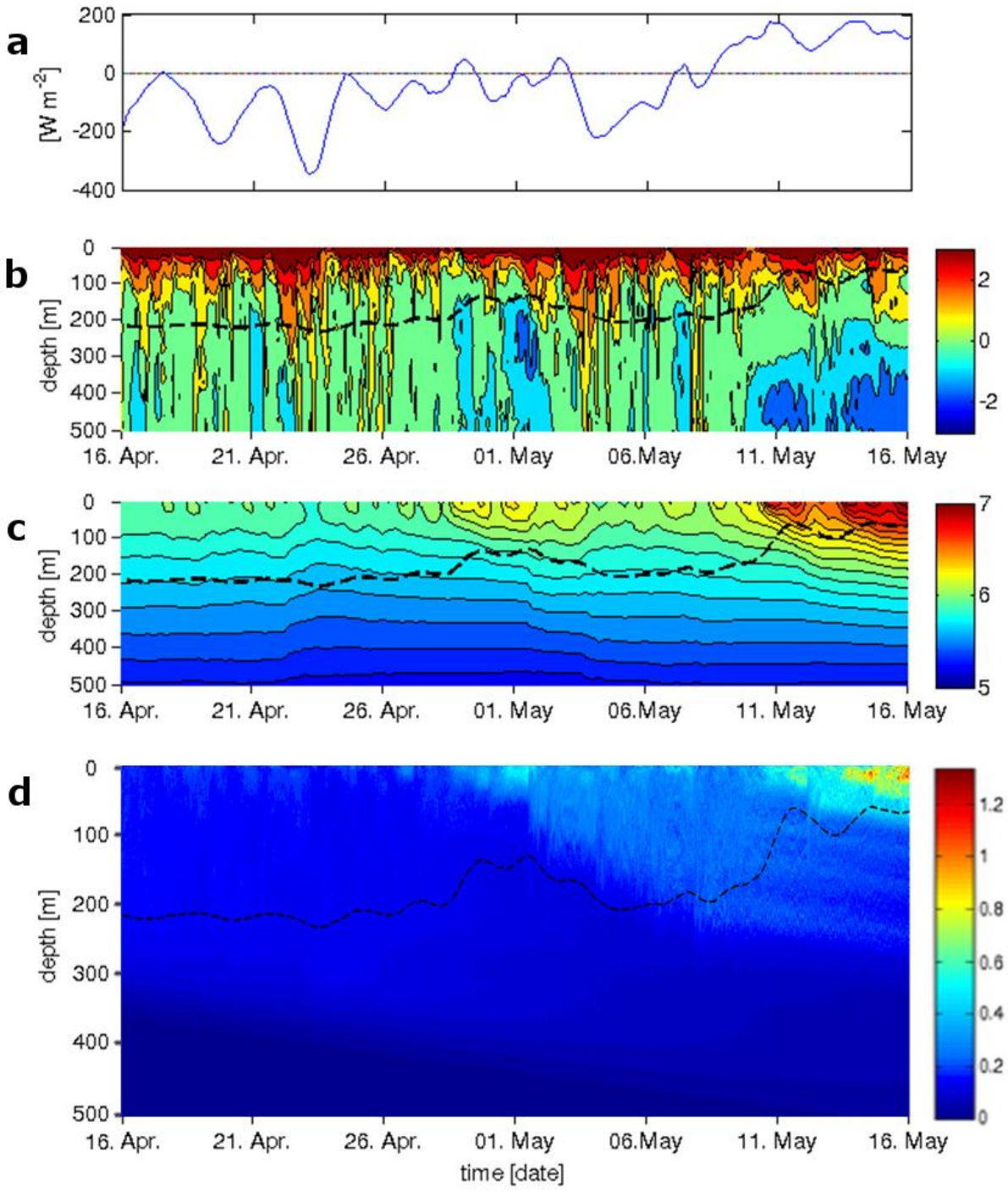

Figure 4 *Time series of (a) net surface heat flux [W m^{-2}] and Hovmoeller diagram showing (b) turbulence (log scale) (c) temperature [°C] and (d) phytoplankton concentration [mg Chl m^{-3}] over the course of the simulation. The black dashed line indicates the estimated mixed layer.*

2 Parameterisation of phytoplankton in deep convection ('phyto-parameterisation')

In order to derive a meaningful 'biological' parameterisation, field data on physiological rates, such as primary productivity, is required. However this data is not available to date. Therefore, as a first step a different parameterisation for the application in hydrostatic ecosystem models was used in the following.
A full description of this parameterisation (incl. equations) with validation and model simulations can be found in Grosse et al. (see Appendix II).

2.1 'phyto-parameterisation'

The basic idea behind the approach is to compensate the lack of convective vertical displacement of phytoplankton by allowing primary production throughout the whole convective mixed layer. This is done by distributing the vertically averaged light limitation within the euphotic zone over the whole mixed layer during winter. To account for summer situations where convection is not present, a transition between the conventional parameterisation and the phyto-convective approach is applied. This is done by using a weighting function using a MLD of 100 meters as a criterion.

2.2 The ecosystem model (ECOHAM4)

The ecosystem in which the 'phyto-parameterisation' was implemented is the ECOHAM4 model (ECOsystem model, HAMburg, version 4; Paetsch and Kuehn 2008) is a three-dimensional (3D) ecosystem model consisting of the hydrodynamic model HAMSOM (HAMburg Shelf Ocean Model; Backhaus 1985) and the biogeochemical model ECOHAM.

The model domain was set to 48°N-64°N, 15°W-12°E using a resolution of 1/5° lat. and 1/3° lon. This resolution is applied to create on average 20x20 km grid cells. The meteorological forcing was calculated from NCEP/NCAR reanalysis data (Kalnay et al., 1996) and was provided as 6-hourly values.

For a detailed description and a full list of the fluxes between the different state variables and the model parameters used, see Lorkowski et al. (2012).

2.3 Ecosystem model simulations

The validation of the model simulation was done for station Rockall Trough (55°3’24”N, 10°1'4"W), since the required depth resolved winter chlorophyll a (chl-a) data was available here. Fig. 5 exemplifies the fit of the simulation using the 'phyto-parameterisation' (hereafter referred to as phytoconvection run) and the simulation using the conventional parameterisation (hereafter referred to as the standard run) to the observed field data.

The two observed profiles show a distinct structure with increased chl-a concentrations ranging between 0.09 mg Chl m^{-3} and 0.14 mg mg Chl m^{-3} in the upper 500 m to 600 m.

Thereunder, concentrations strongly decrease followed by concentrations of about 0.05 mg Chl m^{-3} below the MLD.

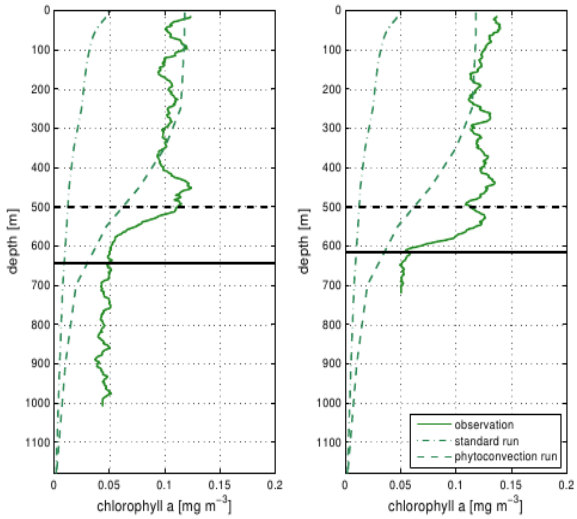

Figure 5 (left): *Comparison of observed (solid) and simulated (dashed/dash-dotted) chlorophyll-a profiles on February 27th, 1996 for the station Rockall Trough. Horizontal black lines depict the MLD referring to the observations (solid) and the simulations (dashed).*

Figure 6 (below): *Hovmoeller diagrams of simulated chlorophyll-a concentrations for (A) the standard run and (B) the phytoconvection run. The dashed lines depict the MLD. The logarithmic color scales should be noticed.*

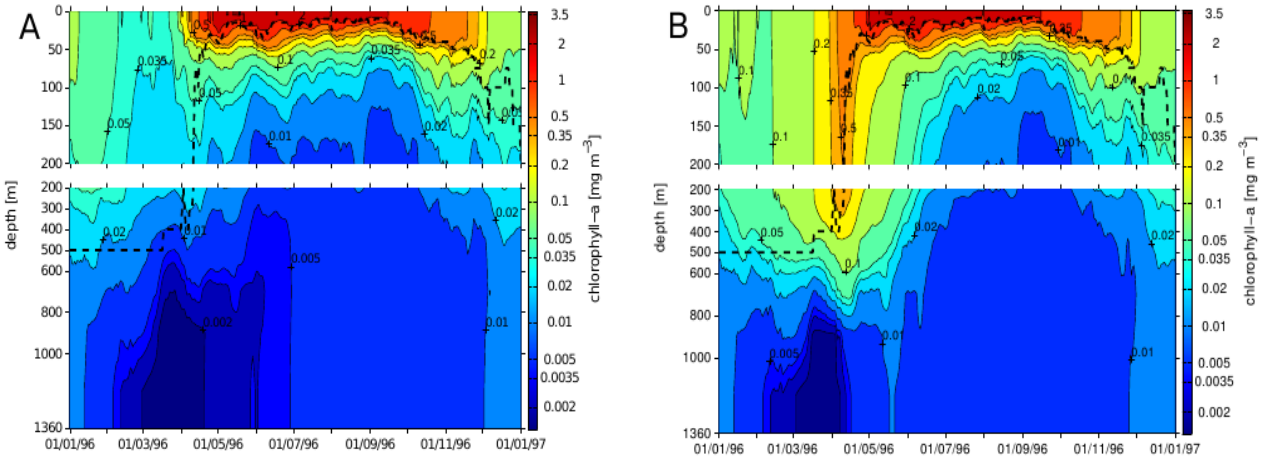

As validation data were only sparsely available the phytoconvection run and the standard run were compared with each other in more detail to show the effects of the 'phyto-parameterisation' on the phytoplankton stock. The temporal development of the total (diatoms and flagellates) chl-a concentration for the two parameterisations at this station is shown in the Howmoeller plot in Fig. 6. The two simulations start from the same initial conditions with highest concentrations of above 0.1 mg chl-a m^{-3} in the upper 100 m and decreasing concentrations in greater depths. For the first two weeks, the two simulations show similarly decreasing concentrations in the upper 100 m and increasing concentrations in the layers below down to the MLD due to downward mixing of the higher surface concentrations.

Thereafter the standard run decreases until late March throughout the whole water column while the phytoconvection run is characterized by steadily increasing concentrations throughout the mixed layer from early February until mid-April. The

concentrations in the standard run drop below 0.05 mg chl-a m^{-3} in the upper 100 m and values less than 0.035 mg chl-a m^{-3} in the deeper layers, while the phytoconvection run shows concentrations of above 0.05 mg chl-a m^{-3} throughout the whole mixed layer and concentrations higher than 0.1 mg chl-a m^{-3} in the upper 200 m to 300 m. Maximum concentrations in the deep part of the winter mixed layer are reached in early April when the MLD declines and a seasonal thermocline develops with values of above 0.35 mg chl-a m^{-3} in the phytoconvection run. At the same time the standard run shows the onset of a strong surface spring bloom indicated by the increase in the chl-a concentrations from less than 0.05 mg chl-a m^{-3} to above 1 mg chl-a m^{-3} within about two weeks. A comparably strong surface bloom is not simulated in the phytoconvection run, because the MLD is still 200 m to 400 m deep, and hence, the phytoconvective parameterisation is fully taken into account.

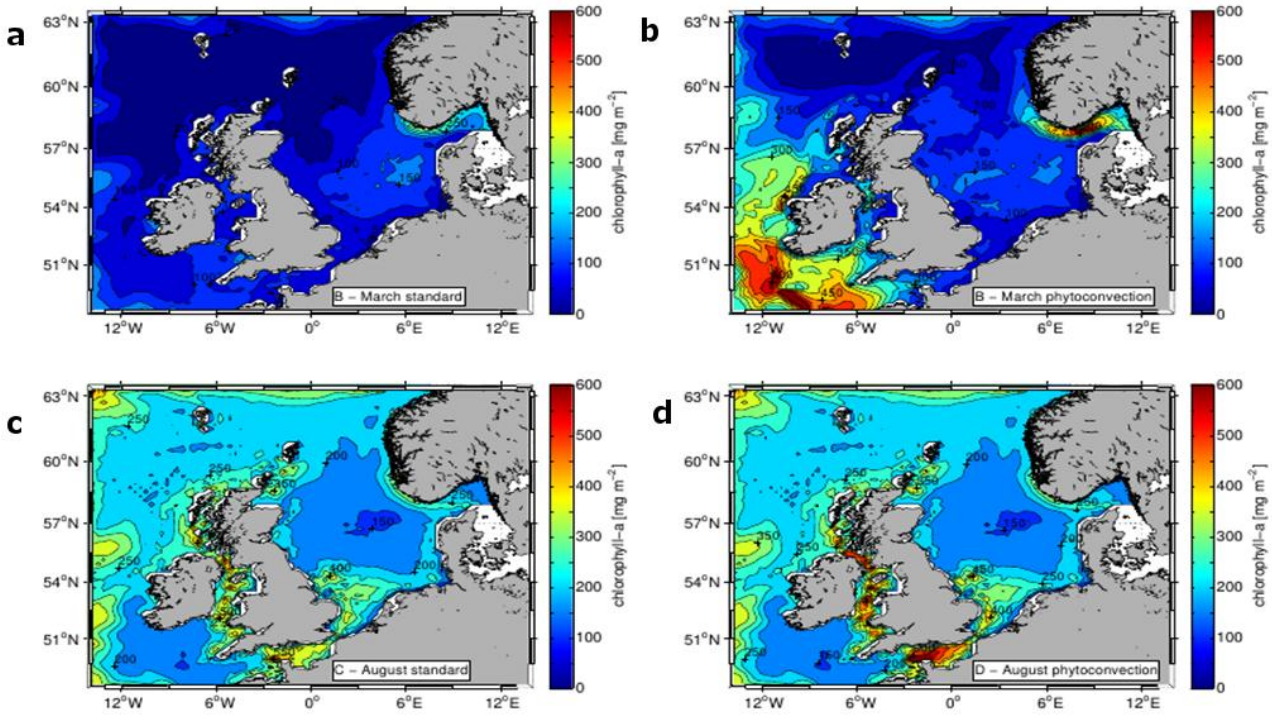

***Figure 7**: Monthly averages of vertically integrated chl-a in the model region for the standard run (a,c) and the phytoconvection run (b,d) for March(a,b) and August (c,d). The integration depth is 500 m.*

In March the vertically integrated, monthly averaged chl-a concentrations of the upper 500 m for the standard run (Fig. 7a) shows significantly lower concentrations than the phytoconvection run (Fig. 7b) in the areas south and west of Ireland. In these areas the MLD is deeper than the reference depth (100 m). The highest concentrations in these regions exceed 600 mg chl-a m^{-2} in the phytoconvection run while the concentrations in the standard run stay below 150 mg mg chl-a m^{-2} in the same area. In the deep areas further north the concentrations in both simulations show similarly low concentrations despite the deep mixed layers. This can be attributed to the very low initial phytoplankton concentrations in the beginning of the simulation. South of Norway the phytoconvection run produces the highest concentrations in the deepest area of the Skagerrak due to the deep mixed layer. In contrast, the standard run shows the highest concentrations directly at the coast caused by the onset of the spring bloom. In the

shallower shelf regions, e.g. the southeastern North Sea the two simulations are in good agreement with each other which is due to the shallow depth (below 100 m). This demonstrates that the weighting function allows the application of the new parameterisation on the shelf.

In August the two simulations show the same patterns and concentrations in most parts of the simulated area. The shallow seasonal mixed layer within the whole model domain causes the switch-off of phytoconvection in the phytoconvection run (Fig. 7d) in these areas. Only in the English Channel and the Irish Sea the phytoconvection run shows significantly higher concentrations than the standard run (Fig. 7c). In these regions tidal mixing and bottom topography lead to strong vertical mixing throughout the whole year, preventing the development of a persistent seasonal mixed layer. Due to bottom depths of around 100 m this leads to a stronger influence of the phyto-parameterisation. This region is known for tidal fronts and related increased phytoplankton production during summer (Pingree et al., 1978), thus indicating reasonable chl-a concentrations simulated in the phytoconvection run in these regions.

3 *The influence of the winter phytoplankton stock on the carbon budget*

The phytoplankton winter stock can potentially have major influences on the air-sea flux of CO2 and the carbon export production. The model simulations were analysed with regard to both.

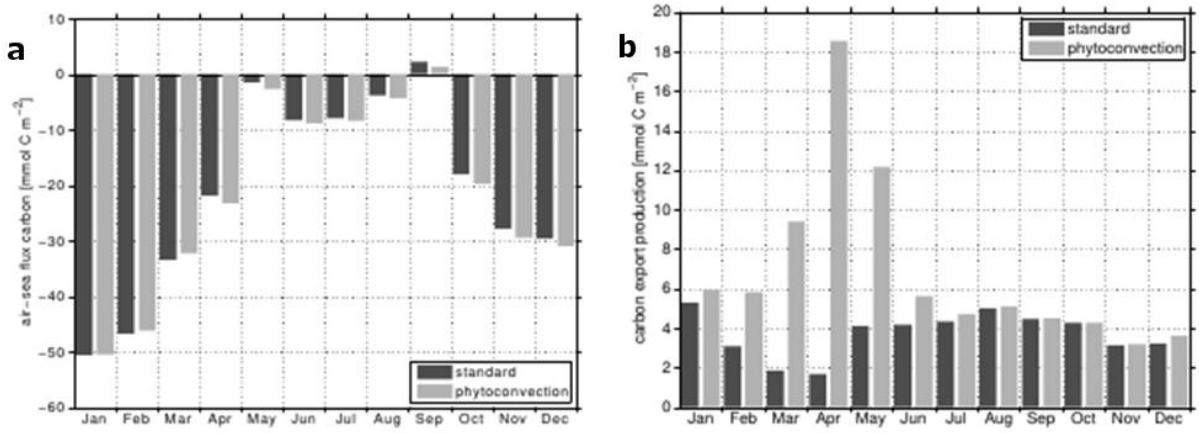

Figure 8: *Time series of monthly integrated (A) air-sea carbon flux and (B) carbon export production for the standard run (dark grey) and the phytoconvection run (light grey). The negative values in the air-sea flux indicate outgassing of CO2. The carbon export production is defined as the fast-sinking detritus sinking below 500 m depth referring to the maximum MLD at the analysed station.*

3.1 *AIr-Sea Carbon Flux (ASCF)*

The analysis of the time series (Fig. 8a) indicates that the influence of the winter phytoplankton stock has a much larger impact on carbon export than on the ASCF. For the ASCF the two simulations are only slightly different from each other throughout the whole seasonal cycle. Outgassing of CO_2 which is indicated by the negative ASCF is strongest during winter induced by the transport of carbon-enriched deep water to the

surface.

Compared to the standard run, the phytoconvection run shows minimally higher values in winter. This is due to the higher phytoplankton biomass, and therefore, increased primary production at the surface. During summer the ASCF stays on a relatively high level due to the ongoing primary production. From October to December outgassing again intensifies due to increased mixing which brings carbon-enriched water to the surface, and the reduced primary production.

3.2 Carbon Export Production (CEP)

Carbon export production was defined as the export of fast-sinking particulate organic matter (POC) below 500 m depth or into the bentos for areas shallower than 500 m. In difference to the ASCF, the CEP shows significant differences in spring between the two simulations (Fig. 8a, Fig. 8b). While the CEP in the standard run steadily decreases from January to April until the spring bloom is fully developed, the phytoconvection run shows a steady increase in the CEP from February to April with maximum amounts being 6 to 9 times higher than in the standard run. This can be attributed to the significantly higher phyto- and zooplankton biomasses in the lower part of the mixed layer, which lead to higher amounts of fast-sinking detritus in the reference depth.

The reduction of the MLD in April leaves a large portion of the phytoplankton biomass below the mixed layer which is then transferred to detritus sinking to the deep ocean, inducing the large peak (18.5 mmol C m^{-2}) of CEP simulated by the phytoconvection run. Similar dynamics have been observed at the Porcupine Abyssal Plane long term observatory (PAP) (Körtzinger et al. 2008) as well as during the North Atlantic Bloom Experiment 2008 (NABE) (Alkine et la. 2012). These dynamics were not captured by the standard run, since the required biomass, stemming from a sustained winter production was not captured.

During the summer period the two simulations showed similar results since the mixing depth was normally below the euphotic depth, except during events of strong wind, and consequently the parameterisation applied was the same.

Starting in autumn the CEP becomes again slightly higher in the phytoconvection run due to the increasing influence of phytoconvection, and hence, the slightly higher concentrations of phytoplankton in greater depths (see Fig. 6).

Generally the spatial distribution of the CEP was strongly related to the phytoplankton biomass. The monthly-averaged daily CEP at 500 m over whole model domain (Fig. 9) showed the strongest influence of the phyto-parameterisation during spring, which is also reflected in Fig. 8.

During this period, the largest difference in absolute values in between the two runs is simulated in the shelf area. However in relative numbers the increase in CEP in the phytoconvection run, in comparison to the standard run, is on the same order of magnitude (~3 fold increase) in the open ocean west of the British Isles.

Often CEP is measured at a fixed depth. However since the common definition of carbon export requires long-term storage, this depth has to exceed the maximum annual mixing depth. Otherwise phytoplankton cells would be recaptured by, for example spring storms, and thus would be re-entrained into the mixed layer (D'Asaro 2008).

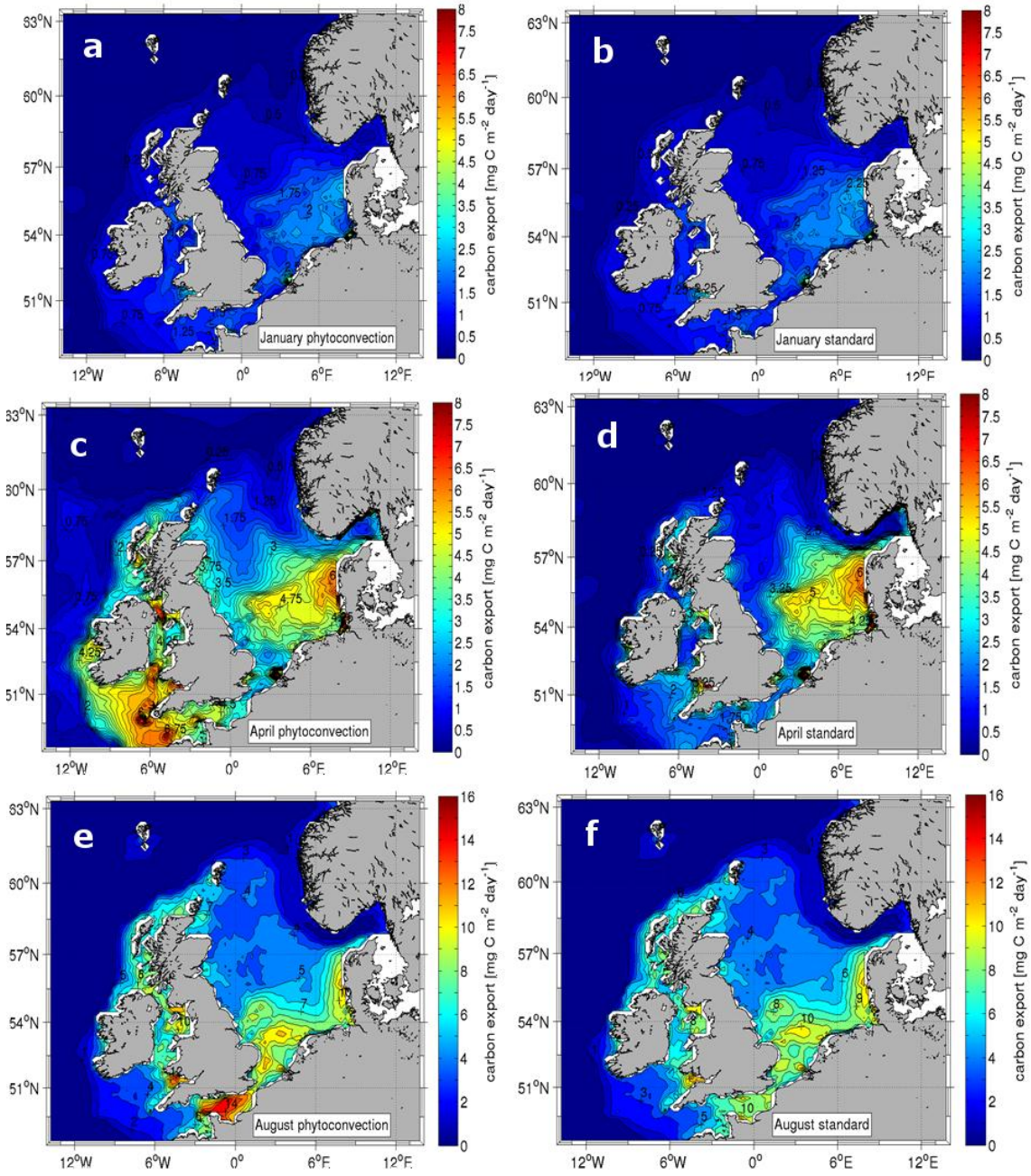

Figure 9: *Monthly averages of daily carbon export production at 500 m depth or into the benthos for areas shallower than 500 m in the model region for the phytoconvection run (a,c,e) and the standard run (b,d,f) for January (a.b), April (c.d) and August (e,f). In areas shallower than 500m the bottom depth was used as the integration depth.*

In order to get an idea of the validity of the used reference depth for carbon export (500 m), carbon export at the annual maximum depth of MLD was estimated (Fig. 10a-e). The maximum MLD is shown in Fig. 10g.

The comparison in between the fixed reference depth and the annual maximum MLD as a reference depth, shows an average annual difference of 2.8 % (max. 7.5% in April) for CEP, while the integrated average annual phytoplankton stock shows a difference of 0.3%.

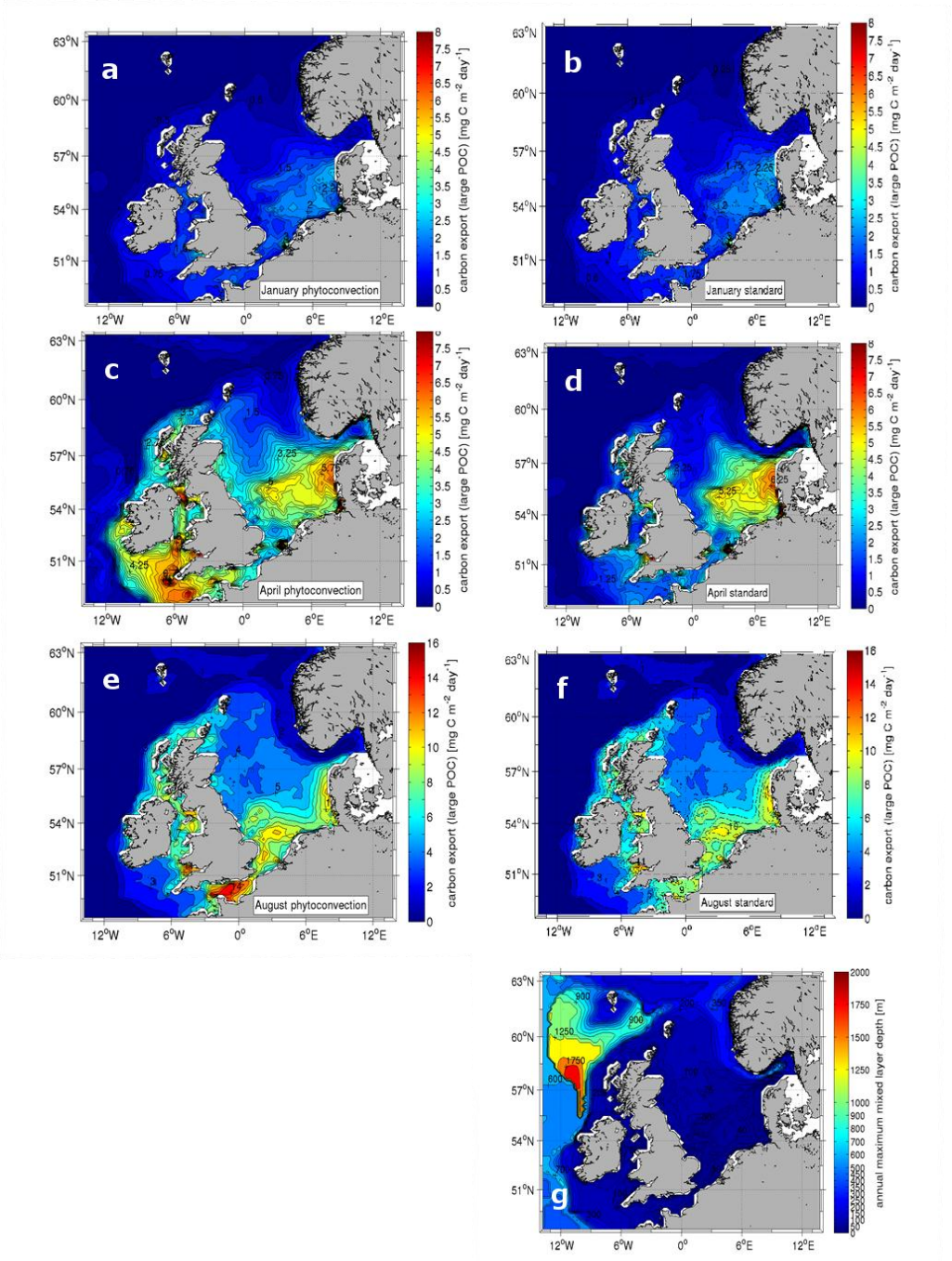

***Figure 10**: Monthly averages of carbon export production at the annual maximum mixed layer depth in the model region for the phytoconvection run (a,c,e) and the standard run (b,d,f) for January (a,b), April (c,d) and August (e,f). In areas shallower than 500m the bottom depth was used. (g) shows the annual maximum mixed layer depth as simulated by the model.*

(max. 2.5 % in December). These differences indicate that the chosen reference depth for the parameterisation, while generally appropriate, has a larger impact on the carbon export than on the integrated phytoplankton biomass. This effect is particularly pronounced in spring, due to the changes in MLD.

4 Conclusions

Deep convection has been suggested to play an important role in winter phytoplankton dynamics in the North Atlantic (Backhaus. et al. 2003). In order to account for this effect in coupled ecosystem models, a simple parameterisation, named 'phytoparameterisation', has been tested. In the open ocean (deeper than 500 meters) the phytoparameterisation led to an overall increase in phytoplankton biomass and CEP in comparison to the standard parameterisation commonly used in ecosystem models. The effect on phytoplankton biomass was strongest during winter with an increasing effect from December to March leading to the largest increase (~150%) during early spring when light conditions became less limiting, but prior to the onset of stratification. The effect on CEP shows almost a Gaussian distribution around the peak in April, a time of the year, during which the reduction in MLD was already occurring in the simulation (Fig. 11). These results can be explained by the retreat of the MLD, leaving a large proportion of the cells below the mixed layer and thus to sink to the deep ocean. This relation has been pointed towards by Evans & Parslow (1985) (even though the general focus of this article is on zooplankton grazing) as well as been observed in the ocean (Körtzinger et al. 2008, Alkire et al. 2012).

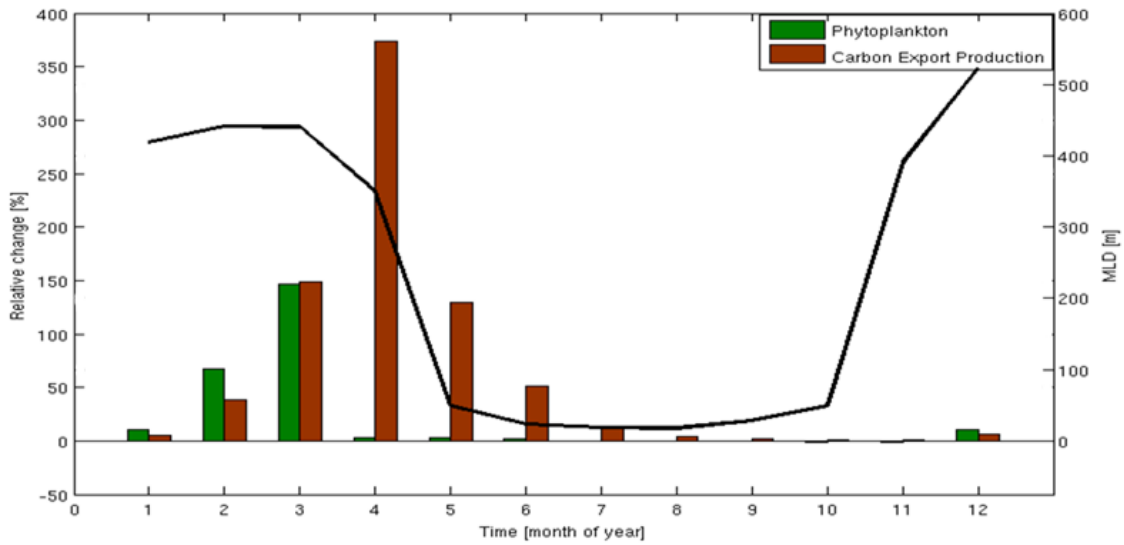

***Figure 11**: Simulated influence, expressed as relative change [%] of the integrated phytoplankton biomass (green, left axes) and carbon export production at 500 m (red, left axes). Also shown is the annual maximum mixed layer depth (black line, right axes) in the open ocean (>500 m depth).*

Summarizing it can be said, that to improve the treatment of winter phytoplankton dynamics, a simple parameterisation has been implemented in an ecosystem model. During winter the 'phytoparameterisation' simulated an increased phytoplankton biomass (up to 150%) and carbon export production (up to over 350%) in comarision to

the conventional approach. These results indicated an underestimated importance of the simulated winter phytoplankton stock on the annual carbon budget and highlight the need to further improve our knowledge about winter phytoplankton dynamics.

4 References

Alkire, M.B., E.A. D'Asaro, C. Lee, M.J. Perry, A. Gray, I. Cetinic, N. Briggs, E. Rehm, E. Kallin. 2012. Estimates of net community production and export using high-resolution, Lagrangian measurements of O2, NO-3, and POC through the evolution of a spring diatom bloom in the North Atlantic. Deep Sea Research Part I 64: 157.

Backhaus, J., 1985. A three-dimensional model for the simulation of shelf sea dynamics. Dtsch. Hydrograf. Z. 38 (4), 165–187.

Backhaus, J. O., Hegseth, E. N., Wehde, H., Irigoien, X., Hatten, K. and Logemann, K. (2003). "Convection and primary production in winter." Marine Ecology Progress Series: 26: 1-14.

Backhaus, J. O. and Kämpf, J. (1999). "Simulations of sub-mesoscale oceanic convection and ice-ocean interactions in the Greenland Sea." Deep Sea Research PartII: Topical Studies in Oceanography 46(6-7): 1427-1455.

Backhaus, J. O., Wehde, H., Hegseth, E. N. and Kämpf, J. (1999). "Phyto-convection": the role of oceanic convection in primary production. Marine Ecology Progress Series189: 77-92.

Bissinger, J. E., Montagnes, D. J. S., Sharples, J. and Atkinson, D. (2008). "Predicting marine phytoplankton maximum growth rates from temperature: Improving on the Eppley curve using quantile regression." Limnology and Oceanography 53(2): 487-493.

Evans Geoffrey T., John S. Parslow, A model of annual plankton cycle. Biol. Ocenaogr. 3, 327-347 (1985)

Falkowski, P. G. and Owens, T. G. (1980). "Light--Shade Adaptation : Two strategies in marine phytoplankton." Plant Physiol. 66(4): 592-595.

D'Asaro, E. A. (2008). "Convection and the seeding of the North Atlantic bloom " Journal of Marine Systems 69(3-4): 233-237.

Grosse, F., C. Lindemann, J. Paetsch, J.O. Backhaus. The influence of deep winter convection on primary production: a parameterisation using a hydrostatic three-dimensional biogeochemical model, Subm. to Journal of Marine Systems

Irigoien, X. and others 1998. A high frequency time series at Weathership M, Norwegian Sea, during the 1997 spring bloom: feeding of adult female Calanus finmarchicus. Marine Ecology Progress Series 172: 127-137.

Jassby, A.D., T. Platt. 1976. Mathematical formulation of the relationship between photosynthesis and light for phytoplankton Limnology and Oceanography 21: 540-547.

Janowiak, J., Mo, K., Ropelewski, C., Wang, J., Leetmaa, A., Reynolds, R., Jenne, R., Joseph, D., 1996. The NCEP/NCAR 40-year reanalysis project. Bull. Am. Meteorol. Soc. 77 (3), 437–471.

Kalnay, E., Kanamitsu, M., Kistler, R., Collins, W., Deaven, D., Gandin, L., Iredell, M., Saha, S., White, G., Woollen, J., Zhu, Y., Chelliah, M., Ebisuzaki, W., Higgins, W., Körtzinger, A. and others 2008. The seasonal pCO2 cycle at 49°N/16.5°W in the northeastern Atlantic Ocean and what it tells us about biological productivity. Journal of Geophysical Research **113:** C04020.

Lorkowski, I., P aesch, J., Moll, A., Kuehn, W., 2012. Interannual variability of carbon fluxes in the North Sea from 1970 to 2006 – Competing effects of abiotic and biotic drivers on the gas-exchange of CO2 . Estuar. Coast. Shelf Sci. 100 (0), 38–57.

McDougall, T. J., Jackett, D. R., Wright, D. G. and Feistel, R. (2003). "Accurate and Computationally Efficient Algorithms for Potential Temperature and Density of Seawater." Journal of Atmospheric and Oceanic Technology 20(5): 730-741.

Niehoff, B., U. Klenkel, H.-J. Hirchel, X. Irigoien, R. Head, and R. Harris. 1999. A high frequency time series at Weathership M, Norwegian Sea, during the 1997 spring bloom: the reproductive biology of Calanus finmarchicus. Marine Ecology Progress Series **176:** 81-92.

Paetsch, J., Kuehn, W., 2008. Nitrogen and carbon cycling in the North Sea and exchange with the North Atlantic–A model study. Part I. Nitrogen budget and fluxes. Cont. Shelf Res. 28 (6), 767–787.

Pingree, R., Holligan, P., Mardell, G., 1978. The effects of vertical stability on phytoplankton distributions in the summer on the northwest European Shelf. Deep Sea Res. 25 (11), 1011–1016.

Sakshaug, E., K. Andresen, and D. A. Kiefer. 1989. A Steady State Description of Growth and Light Absorption in the Marine Planktonic Diatom Skeletonema costatum. Limnology and Oceanography 34: 198-205.

Waite, A. M., P. A. Thompson, and P. J. Harrison. 1992. Does energy control the sinking rates of marine diatoms? Limnology and Oceanography 37: 468-477.

Wehde, H. and Backhaus, J. O. (2000). "The fate of Lagrangian tracers in oceanic convective conditions: on the influence of oceanic convection in primary production."Nonlinear Analysis: Real World Applications 1: 3-21.

Wehde, H., Backhaus, J. O. and Nøst Hegseth, E. (2001). "The influence of oceanic convection in primary production." Ecological Modelling 138(1-3): 115-126.

Appendix I

Individual-based model (IBM)

We did not aim at a biological model with high physiological detail. The approach taken rather used a simple model, able to capture the dynamics of the system and showing the underlying mechanism. By doing so, we hoped to avoid limiting the applicability of this model study to specific small scale regional, temporal conditions or to specific phytoplankton groups (e.g. diatoms or dinoflagellates). The biological IBM employed here describes the dynamics of the phytoplankton cells within the ocean slice. Individual cells represent Lagrangian tracers in the CM which, besides their sinking rate, are affected by the hydrodynamics in the same way as water, consequentially following the convective circulation. Each Lagrangian tracer in the model can be visualized as representing an ensemble of phytoplankton cells of indefinite size and biomass. According to Liebig's law of the minimum, which states that the growth rate is controlled by the most limiting resource, phytoplankton growth during winter in the North Atlantic is controlled by light, while nutrients are plentiful. Even though grazing during the winter is possible, the influence is minimal due to the relatively low abundance of active grazers at this time. For these reasons, and to reduce model complexity, nutrients and grazing are neglected in this study (although the effects of possible low grazing were included in the mortality estimate).

The change of biomass (B) is dependent on growth (μ), respiration (r) and mortality (m):

$$\frac{\partial B}{\partial t} = B\,(\mu - r - m) \tag{1}$$

Light- and temperature-dependent gross growth (μ) is then calculated by

$$\mu = \mu_{max}\ PL(z) \tag{2}$$

where μ_{max} is the maximum growth rate dependent upon the temperature, using the modified Eppley-curve formulation by (Bissinger et al. 2008):

$$\mu_{\max} = 0.81\ e^{0.063\ temp} \tag{3}$$

with *temp* denoting temperature in degree Celsius [°C]. $PL_{(z)}$ represents the production light factor at depth z according to (Jassby & Platt 1976). PAR(z) describes the exponentially decreasing photosynthetically active radiation (PAR) at depth z according to:

$$PAR(z) = I_0\ k_{par}\ e^{-k_e z} \tag{4}$$

where k_{par} is a constant set to 0.43 representing the percentage of the light spectrum that is used for photosynthesis (e.g. Ryther (1956)) and I0 is the incoming radiation at the sea surface, z is the depth, k_e (0.04 m^{-1}) is the extinction coefficient due to turbidity. Self-shading by phytoplankton cells is not considered here as it only plays a significant role at higher phytoplankton concentrations or in turbid waters.

Adopting the approach by Sakshaug et al. (1989), the respiration rate was assumed to be 12% of μmax, based on Falkowski and Owens (1980) who showed that light/shade adapted phytoplankton cells acclimatize their dark respiration rate to different light regimes proportional to their gross primary production. Following this relationship we model dark respiration as a function of gross primary production. To exclude the possibility of the dark respiration rate reaching zero an arbitrary lower limit of 0.5% of the maximal respiration is applied.

The sinking rate of each cell has been calculated for each time step, based on the concept by Waite et al. (1992), who coupled the sinking rate to the overall metabolic state of the cell. They found that if after light exposure, cells where put into the dark their sinking rate could be described as a negative function of their respiration rate, which is in agreement with earlier studies (Weger et al. 1989). We adjusted the sinking rate to yield realistic values under the given conditions:

$$s = -(3.5\, e^{11\, r}) \tag{5}$$

with r being the average respiration rate over the last 12 hours.
As sinking and respiration are accounted for in our model, mortality rate represents the other loss terms e.g. potential grazing pressure or programmed cell death (PCD) and is set to of 0.05 d^{-1} of total production (Backhaus et al. 1999). A list of the variables and parameters used in the model is given in Table 1 and Table 2, respectively.